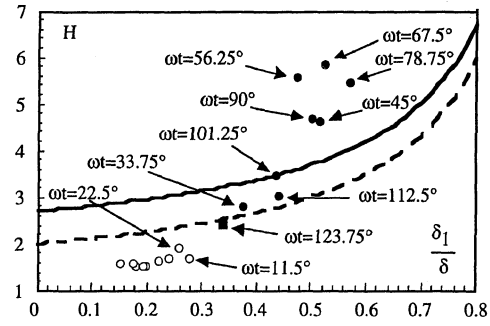

Fig. 3 Separation criterion in pitching motion. Sandborn and Kline's[5] criterion: ——, fully developed separation and – – –, intermittent separation. Experiments: ○, attached flow: 0 deg < ωt < 22.5 deg; ωt = 135 deg; 281.25 deg < ωt < 360 deg; ■, intermittent reattachment: ωt = 123.75 deg; and ●, fully developed separation: 33.75 deg < ωt < 123.75 deg.

have clearly pointed out that the transition, the separation, and the reattachment process are delayed as k increases. Moreover, it is possible to determine all along the period the nature of the boundary layer (attached, separated, near separation, or reattachment) by analyzing the simultaneous evolution of the u tangential profile and turbulence intensity σ_u obtained by the ELV method.[4]

From such results, it can also be concluded that the duration of the separation along the oscillation period is shown to decrease when the reduced frequency k increases.

In steady flow regimes, the Sandborn and Kline[5] criterion is based on the shape factor H, which is expressed as a function of δ_1/δ,

$$H_{\text{sep}} = A + \left[\frac{1}{1-(\delta_1/\delta)}\right] \tag{3}$$

Such a criterion, which appears also to be able to differentiate intermittent separations ($A = 1$) (for more than 5% of the time the flow moves upstream, $u < 0$) from fully developed separations ($A = 1.70$) (for more than 50% of the time the flow moves upstream, $u < 0$), has been applied successfully to characterize the boundary-layer separation on the airfoil in steady flow configurations. Moreover, this steady flow configuration study has shown that the reattachment process is also affected by the intermittency phenomenon.[4]

Because of the similarity observed on the (U, V, σ_u) profiles during the separation process occurring on the NACA 0012 airfoil in either steady flow or pitching motion,[6] an attempt to check the Sandborn and Kline[5] separation criterion has been made in this study. An example of an application of this criterion is shown in Fig. 3 for the pitching motion case corresponding to $k = 0.283$. The Sandborn and Kline criterion appears to be well suited to delimiting the attached boundary-layer regime (open symbols) and the separated flow regimes (solid symbols) in the unsteady flow generated by the pitching motion. However, within the separated zone the criterion appears to be less efficient in differentiating the intermittent separation from the fully developed separation. In Fig. 3, the fully developed separation is identified by the criterion as an intermittent type separation at $\omega t = 33.75$ deg.

Conclusion

In the present study, the ELV method has been successfully extended to two-dimensional velocity measurements (u, v) around moving curved walls and airfoils oscillating in pitching motion.

The transition criterion previously established on an oscillating flat-plate model is also shown to be valid on the NACA 0012 airfoil either in steady flow or in pitching motion, at least under our experimental conditions.

Concerning the separation/reattachment process, the Sandborn and Kline criterion appears to be well suited to delimiting attached and separated flow regimes. A refinement of this criterion seems to be required for differentiating intermittent and fully separated regimes. Moreover, the cyclic separation/reattachment process is shown to be strongly influenced by the reduced frequency parameter k.

The increase of the frequency k is shown to produce a time delay on the transition, separation, and reattachment processes.

Acknowledgments

The authors are thankful for the support provided by the "Direction des Recherches, Etudes et Techniques" under Grants 87/272 and 91/158.

References

[1]Favier, D., Maresca, C., Renon, P., and Autric, J. M., "Boundary-Layer Measurements on Oscillating Models Using an Optical Fibre LDA Technique," *Proceedings of the Sixth International Symposium on Applications of Laser Techniques to Fluid Mechanics*, Durao Edit., Lisbon, Portugal, 1992, pp. 1341–1346.

[2]Pascazio, M., Autric, J. M., Favier, D., and Maresca, C., "Etude de la Couche Limite sur une Plaque Plane Oscillant en Tangage par Vélocimétrie Laser Embarquée," *Proceedings of the Eleventh French Congress of Mechanics*, Dyment Edit., Lille, France, 1993, pp. 253–257.

[3]Favier, D., Maresca, C., and Pascazio, M., "Etude Expérimentale et Numérique du Décollement de la Couche Limite Instationnaire sur un Modèle Oscillant en Ecoulement 2D/3D," Direction des Recherches Etudes et Techniques, Contract 91/158, Synthesis Rept., Paris, Oct. 1994.

[4]Pascazio, M., "Contribution Experimentale et Numérique de la Couche Limite se Développant sur un Profil d'Aile Oscillant: Phénomènes de Transition et de Décollement en Ecoulement Instationnaire," Ph.D. Thesis, Dept. of Mechanics, Univ. of Aix, Marseille II, France, 1995.

[5]Sandborn, V. A., and Kline, S. J., "Flow Models in Boundary Layer Stall Conception," *Journal of Basic Engineering*, 1961, pp. 317–327.

[6]Pascazio, M., Autric, J. M., Favier, D., and Maresca, C., "Unsteady Boundary-Layer Measurement on Oscillating Airfoils: Transition and Separation Phenomena in Pitching Motion," *Proceedings of the AIAA 34th Aerospace Sciences Meeting* (Reno, NV), AIAA, Washington, DC, 1996 (AIAA Paper 96-0035).

Numerical Simulation of Vortex-Induced Oblique Shock-Wave Distortion

Donald P. Rizzetta*
U.S. Air Force Wright Laboratory,
Wright–Patterson Air Force Base, Ohio 45433-7913

Introduction

INTERSECTIONS between streamwise vortices and oblique shock waves occur in a number of practical situations and commonly result in complex three-dimensional flowfields. These events typically involve vortices that are produced by the fore bodies and lifting surfaces of supersonic vehicles or by the tips of canards, fins, and wings. Such vortices then interact with the associated shock-wave systems present over wings or control surfaces, or within high-speed inlets, and may result in loss of lift, increased drag, adverse stability and control, or decreased engine performance. When the interactions are sufficiently strong, vortex breakdown can be induced.

Previous experimental and numerical investigations of shock-wave/vortex interactions are reviewed in Ref. 1. Of these, only the computations of Rizzetta[2] attempted to provide a direct comparison between numerical calculations and experimental data. It was indicated that although solutions to the Euler equations compared reasonably well with measurements in a number of cases, they could not reproduce the vortex breakdown that was often observed experimentally. The purpose of the present work is to simulate oblique shock-wave/wing-tip vortex interactions via solution to the compressible three-dimensional mass-averaged turbulent

Received Dec. 27, 1995; presented as Paper 96-0039 at the AIAA 34th Aerospace Sciences Meeting, Reno, NV, Jan. 15–18, 1996; revision received Oct. 1, 1996; accepted for publication Oct. 4, 1996; also published in *AIAA Journal on Disc*, Volume 2, Number 2. This paper is declared a work of the U.S. Government and is not subject to copyright protection in the United States.

*Research Aerospace Engineer, Computational Fluid Dynamics Research Branch, Aeromechanics Division. Associate Fellow AIAA.

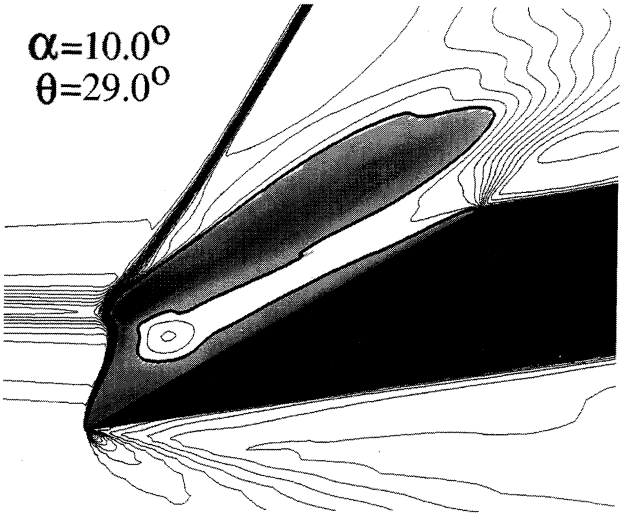

Fig. 1 Mach number contours near the wing midspan for $\alpha = 10.0$ deg and $\theta = 29.0$ deg.

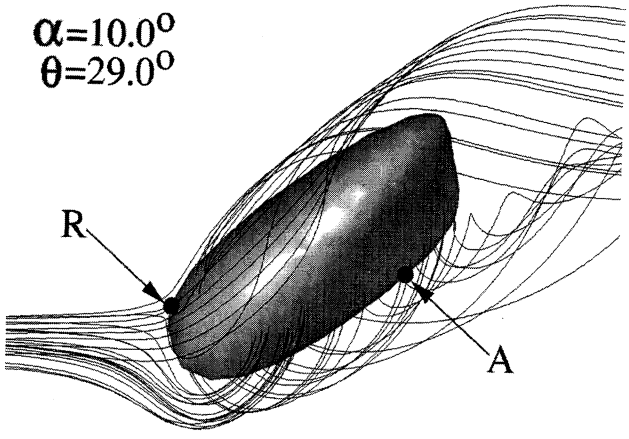

Fig. 2 Particle paths and isosurface of $u = 0$ for $\alpha = 10.0$ deg and $\theta = 29.0$ deg.

Navier–Stokes equations. A two-equation (k-ϵ) turbulence model[3,4] is employed that includes low-Reynolds-number terms and a compressibility correction.[5]

Results

The configuration corresponds to the experiment of Smart and Kalkhoran[6] and consists of airflow past a vertical rectangular fin at a Mach number of 2.49 and chord Reynolds number of 2.17×10^6. A finite span wing having a two-dimensional wedge section is located downstream and produces a shock wave that is intersected by the streamwise vortex generated at the tip of the fin. A complete description of the calculations, including the governing equations, numerical procedure, generation of meshes, boundary conditions, details of the computations, grid resolution and damping coefficient studies, features of the flowfield, and comprehensive results, may be found in Ref. 1. In addition, a previous corresponding computation that considered only the vortex generator tip flow appears in Ref. 7.

Mach number contours in a cross plane near the wing midspan are shown in Fig. 1 for $\alpha = 10.0$ deg and $\theta = 29.0$ deg, where α is the vortex generator angle of attack and θ is the inclination of the wing upper surface. Above the wing leading edge, the vortex impingement and shock-wave distortion are evident, resulting in a shock surface that locally is normal to the oncoming stream. As was pointed out in Ref. 2, this shock distortion is promoted by both the swirl velocity component and the defect in the streamwise velocity component of the vortex core flow. Shaded contours delineate the subsonic flow regions behind the point of the vortex/shock intersection and adjacent to the wing surface. The shock-produced subsonic flow region is seen to be quite large, extending beyond the downstream expansion corner. Most of the postshock reduction in Mach number was incurred by a decrease in the vortex streamwise velocity component. The circumferential component was affected to a lesser degree.

Also in this case, the shock is normal at the wing leading edge and close to becoming detached, in part due to the vortex-induced distortion. This is not unexpected because at the given flow conditions the maximum theoretical inviscid deflection angle for an attached oblique shock wave is approximately 29.7 deg.

Particle paths of the vortex core flow and the isosurface of $u = 0$ appear in Fig. 2, illustrating breakdown of the vortex. Here, u is the

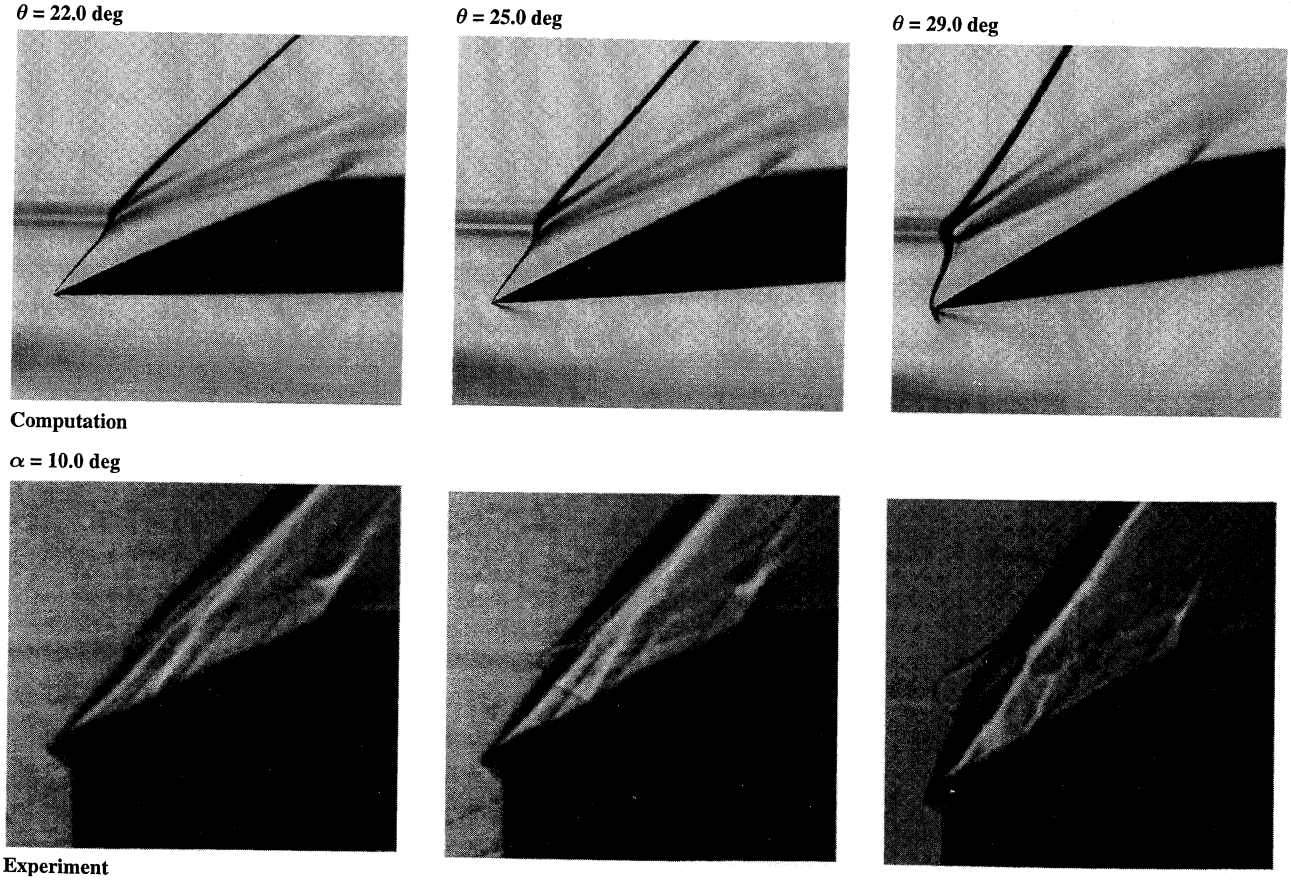

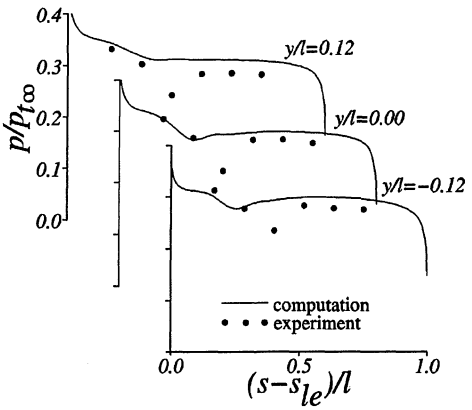

Fig. 4 Wing surface static pressure distributions for α = 10.0 deg and θ = 29.0 deg.

streamwise velocity component and vortex breakdown is defined by the appearance of an off-surface region for which $u < 0$. Unlike subsonic vortex breakdown, in the supersonic case the extent of vortex radial expansion is confined to a moderately small region surrounding the core. Two topological critical points[8] are located on the $u = 0$ isosurface. These are designated in Fig. 2 by R for the upstream repelling spiral saddle (unstable focus/compressing), and by A for the downstream attracting spiral saddle (stable focus/stretching).

Visual comparisons between numerical solutions and experimental shadowgraph images are provided in Fig. 3 for $\alpha = 10.0$ deg and $\theta = 22.0$, 25.0, and 29.0 deg. The numerical results are presented in terms of the magnitude of the density gradient. Many of the same physical features, including the vortex and the distorted shock wave, are evident in both the experimental and computational representations. For $\theta = 22.0$ and 25.0 deg, the numerically simulated distorted shock wave appears much like the experimental image. With $\theta = 29.0$ deg, however, the shock distortion is observed to be more significant in the experimental case. This implies that the numerical simulation predicts a weaker interaction than that which is produced experimentally. Vortex breakdown was predicted numerically only for $\theta = 29.0$ deg.

Calculated static pressure distributions on the wing upper surface for $\alpha = 10.0$ deg and $\theta = 29.0$ deg are compared with experimental data in Fig. 4. In Fig. 4, p is the static pressure, $p_{t\infty}$ the freestream total pressure, s the distance along the inclined wing upper surface whose leading edge is at s_{le}, and l the length of the inclined surface. Generally, the computations predict higher pressure levels than the experiment at all spanwise stations, y/l. The measured pressure deficit near $(s - s_{le})/l = 0.4$ is not duplicated by the computations, which is consistent with the simulated interaction being weaker than the physical interaction as was noted in Fig. 3.

Summary and Conclusions

Steady high-Reynolds-number supersonic flowfields were generated numerically to simulate the interaction between a streamwise wing-tip vortex and an oblique shock wave by solution of the turbulent Navier–Stokes equations. A k-ϵ closure model, which included low-Reynolds-number terms and a compressibility correction, was employed to account for effects of turbulence.

For weaker interactions than those presented here, which did not result in vortex breakdown, calculations agreed reasonably well with the data. When breakdown occurred, the numerically simulated interaction was not as strong as the experimental counterpart. This deficiency is attributed to the inability of the k-ϵ equations to accurately simulate formation of the tip vortex. In particular, it has been shown that the turbulence model could not reproduce the experimentally measured core deficit in streamwise Mach number,[7] which is considered to be crucial to vortex breakdown in this case. Numerical reproduction of strong tip-vortex/shock-wave interaction thus appears to be limited by lack of adequate turbulence modeling for such flows at high Reynolds numbers.

Acknowledgments

Computational resources for the work presented here were supported in part by a grant of supercomputer time from the U.S. Department of Defense Major Shared Resource Centers at Vicksburg and Bay St. Louis, Mississippi. The author is indebted to I. M. Kalkhoran and M. K. Smart for their assistance and cooperation in supplying details and results of the experiment. A number of helpful conversations with M. R. Visbal and R. E. Gordnier are gratefully acknowledged.

References

[1]Rizzetta, D. P., "Numerical Simulation of Vortex Induced Oblique Shock-Wave Distortion," AIAA Paper 96-0039, Jan. 1996.

[2]Rizzetta, D. P., "Numerical Simulation of Oblique Shock-Wave/Vortex Interaction," *AIAA Journal*, Vol. 33, No. 8, 1995, pp. 1441–1446.

[3]Jones, W. P., and Launder, B. E., "The Prediction of Laminarization with a Two-Equation Model of Turbulence," *International Journal of Heat and Mass Transfer*, Vol. 15, No. 2, 1972, pp. 301–314.

[4]Jones, W. P., and Launder, B. E., "The Calculation of Low-Reynolds-Number Phenomena with a Two-Equation Model of Turbulence," *International Journal of Heat and Mass Transfer*, Vol. 16, No. 6, 1973, pp. 1119–1130.

[5]Sarkar, S., Erlebacher, G., Hussaini, M. Y., and Kreiss, H. O., "The Analysis and Modelling of Dilatational Terms in Compressible Turbulence," *Journal of Fluid Mechanics*, Vol. 227, June 1991, pp. 473–493.

[6]Smart, M. K., and Kalkhoran, I. M., "Effect of Shock Strength on Oblique Shock-Wave/Vortex Interaction," *AIAA Journal*, Vol. 33, No. 11, 1995, pp. 2137–2143.

[7]Rizzetta, D. P., "Numerical Investigation of Supersonic Wing-Tip Vortices," *AIAA Journal*, Vol. 34, No. 6, 1996, pp. 1203–1208.

[8]Chong, M. S., Perry, A. E., and Cantwell, B. J., "A General Classification of Three-Dimensional Flow Fields," *Physics of Fluids A*, Vol. 2, No. 5, 1990, pp. 765–777.